

# The whole ball of wax: 3D raypath interferometry from start to *finish*

David C. Henley\*  
dhenley@ucalgary.ca

## Introduction:

**Raypath interferometry** was developed to apply surface corrections to seismic data by estimating and removing '**surface functions**' using an interferometric process. The original 2D version used the **Radial Trace (RT) Transform** to map seismic data from the X/T domain to the common-raypath domain; but **the Tau-P Transform** has recently been shown to be equally suitable. **Raypath interferometry has been successfully applied to both PP and PS data**, and is particularly useful for the latter, since **its corrections are non-stationary**, thus conforming to theory for converted-wave data.

**Extending** raypath interferometry to handle **3D seismic data is not totally straightforward**, since 3D seismic acquisition generally uses **cartesian geometry**, and the most natural way to implement 3D raypath interferometry is based on **radial geometry**.

## 3D considerations

Earlier, we introduced **3D surface functions**, dependent upon surface location, raypath incidence angle, and source-receiver azimuth, and showed how to bin 3D seismic data from **cartesian** gathers, into ensembles compatible with transforming to and from an **azimuthal common-raypath domain**, where the functions are estimated and removed.

We discovered early in the 3D work that our **2D RT Transform is inadequate** for 3D, since it does not accurately restore **trace headers** for ensembles with non-linear source-receiver offset distributions (Figure 1).

This situation forced us to use the **Tau-P Transform** instead, where the challenge was the very large files associated with the required high-resolution Tau-P domain trace ensembles (Figures 2 and 3).

## Ultimate success:

Having chosen the Tau-P Transform, we applied the full **3D raypath interferometry** method to the PP component of the 1995 Blackfoot 3D 3C survey, resulting in a 3D CMP-stacked data volume, of which we show here some **2D slices**, both in the **inline** and **crossline** directions (**to verify that the method is truly 3D**). The main difficulty was providing enough intermediate file space (1 Tbyte) to perform each step.

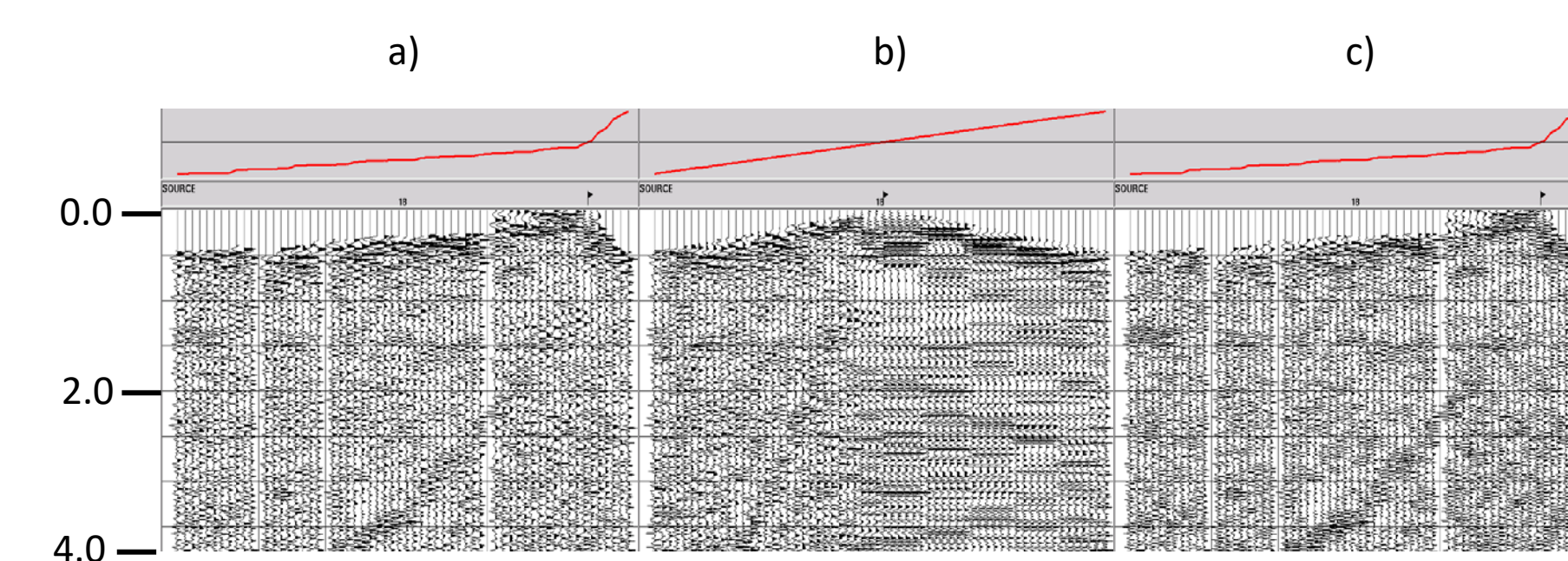


FIG. 1. (a) Original trace ensemble with non-linear source-receiver offsets, (b) Trace ensemble after forward/inverse RT Transform, (c) Trace ensemble after forward/inverse Tau-P Transform.

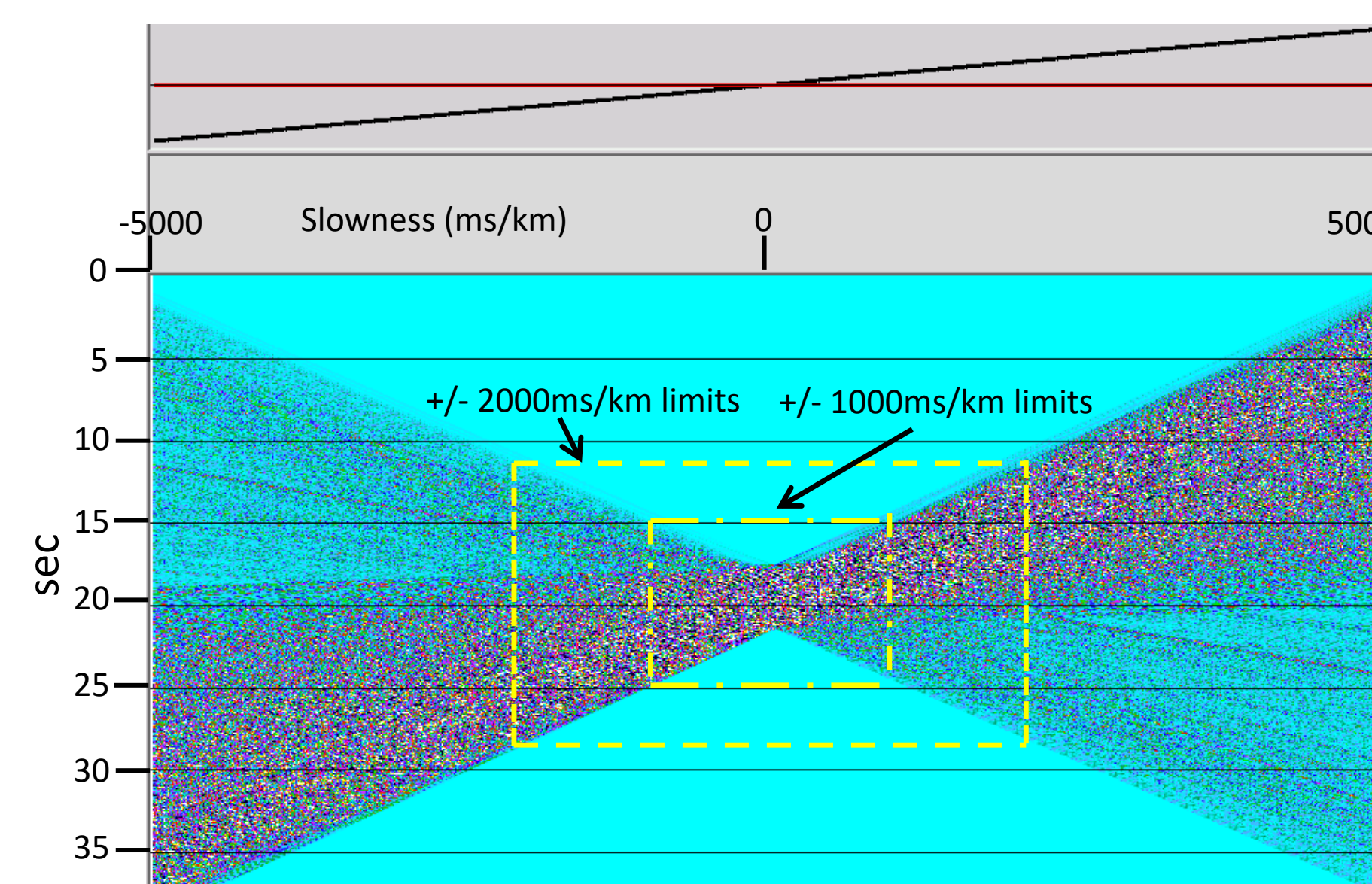


FIG. 2. Tau-P Transform of a typical 3D X/T trace ensemble, requiring nearly **100 times the file space of the original ensemble**. Yellow boxes show the reduction in size if slowness limits are relaxed—but this **reduces Tau-P resolution** unacceptably.

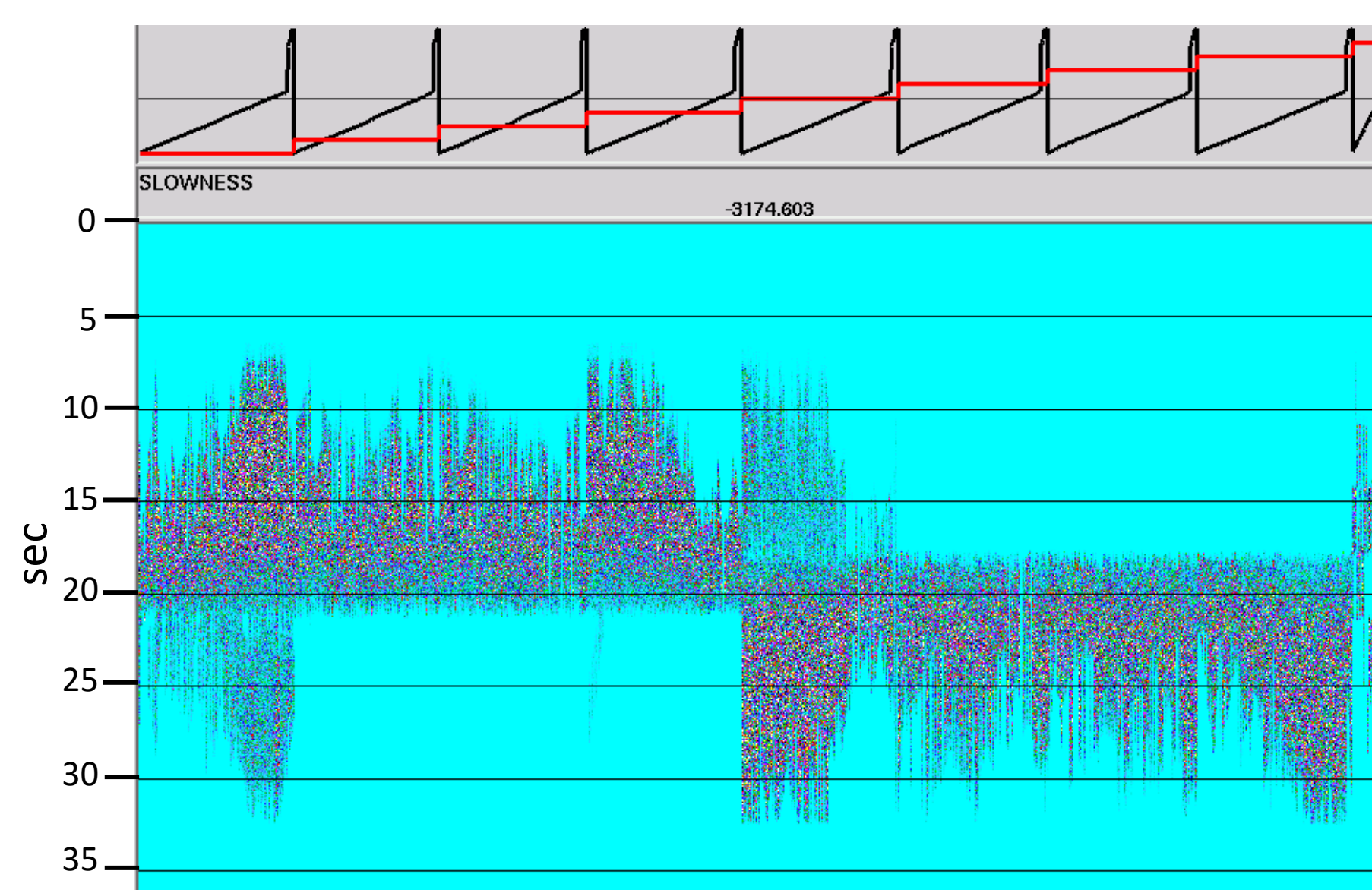


FIG. 3. A typical common-ray-parameter trace ensemble in the Tau-P domain. **There are more than 20,000 traces in this ensemble, each 37sec in length; this is only one of 631 similar ensembles for this data set.**

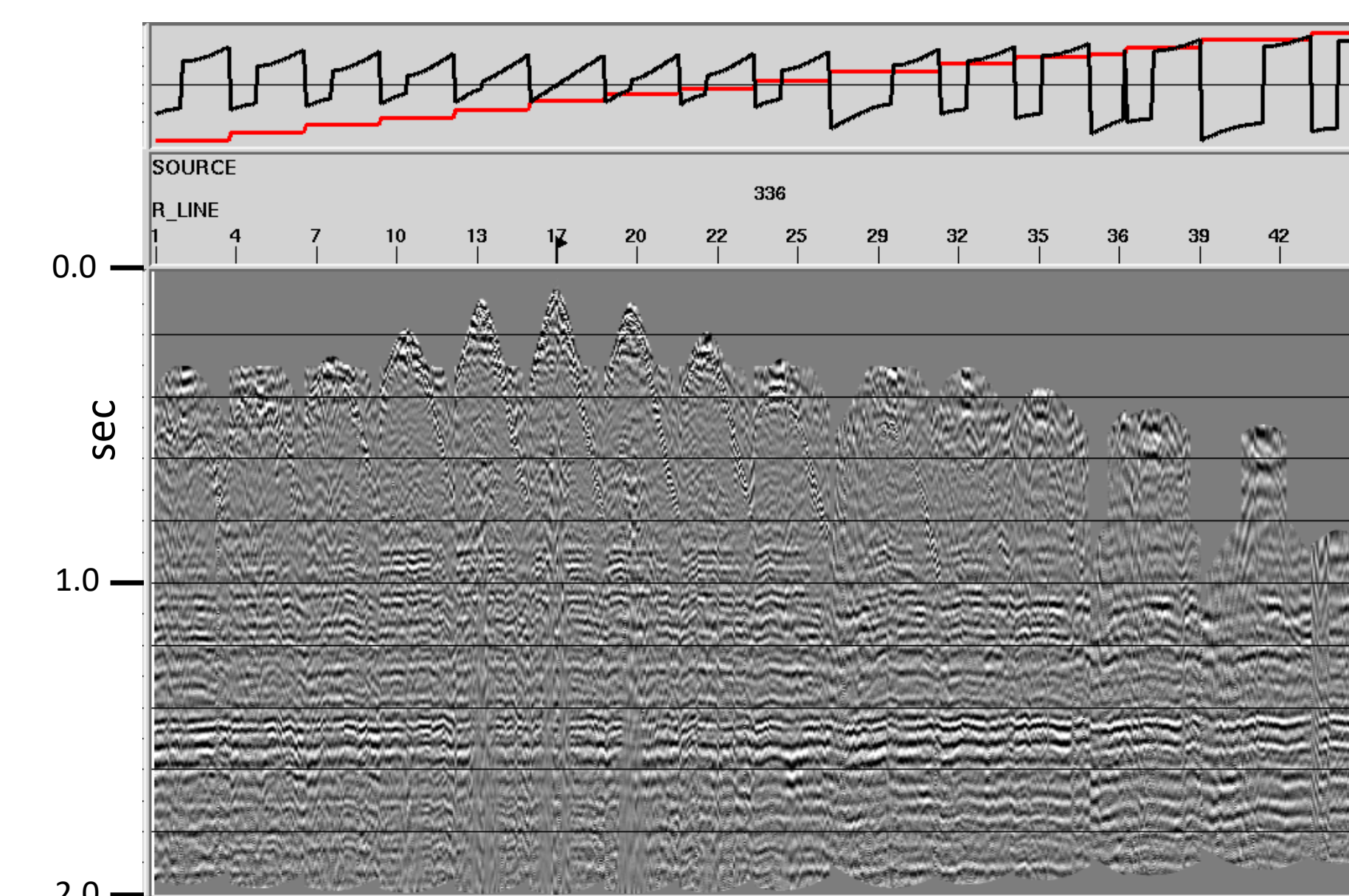


FIG. 4. One source gather from the Blackfoot PP component, sorted by receiver line, NMO applied, no statics applied.

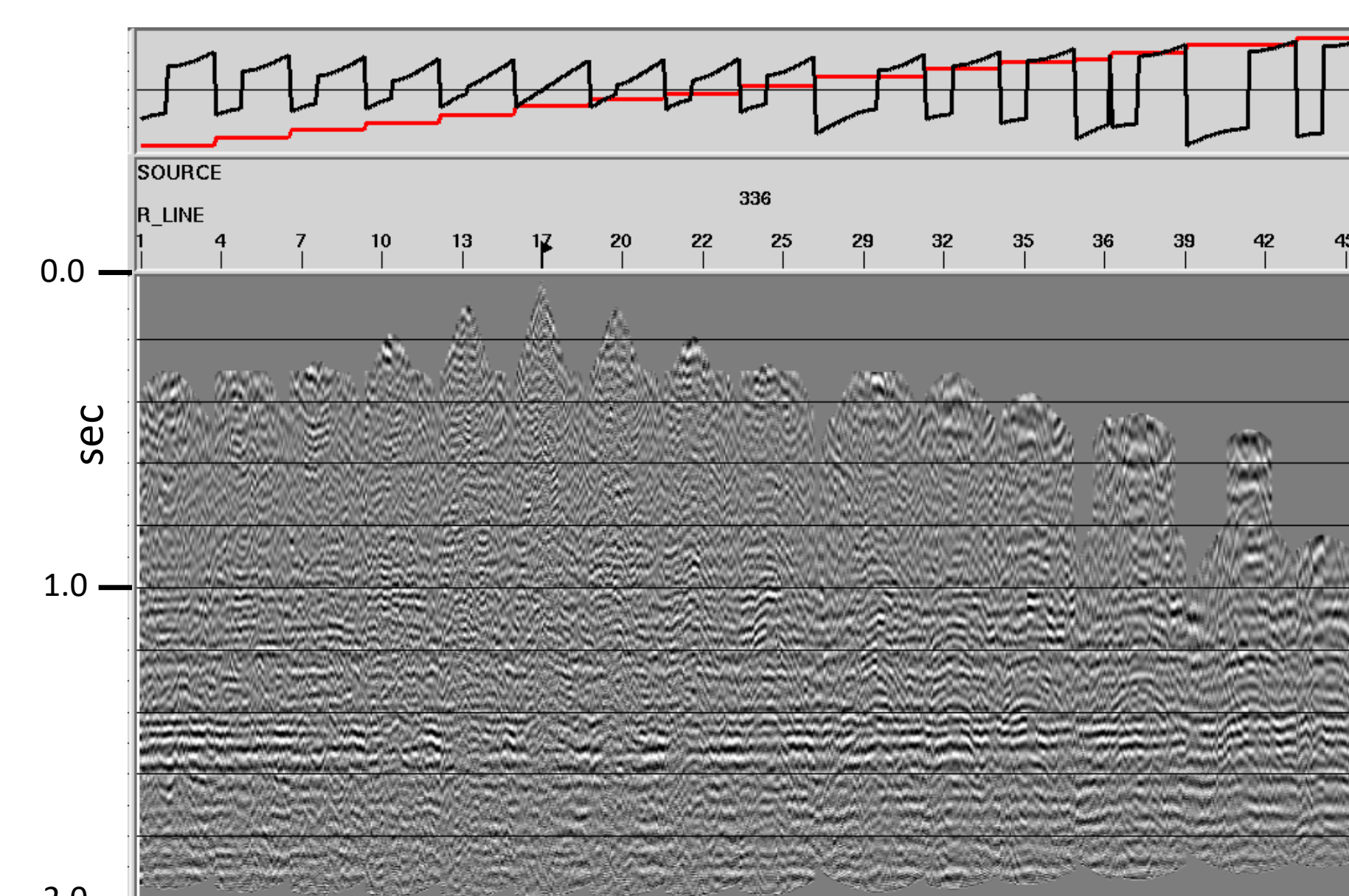


FIG. 5. Source gather from Figure 4, NMO applied, after **3D raypath interferometry**.

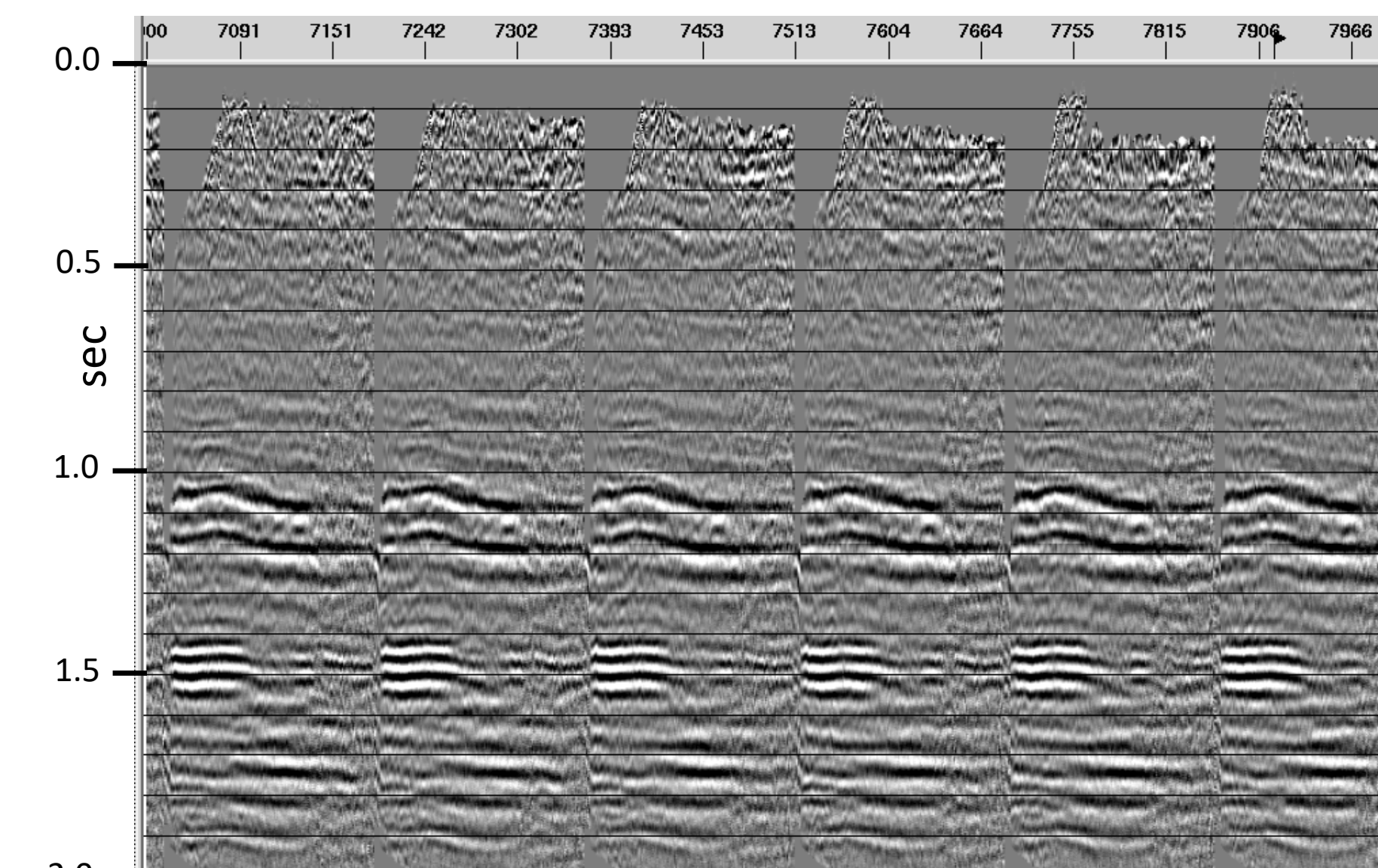


FIG. 6. Six 2D inline slices from the 3D CMP-stacked Blackfoot data volume—no statics applied.

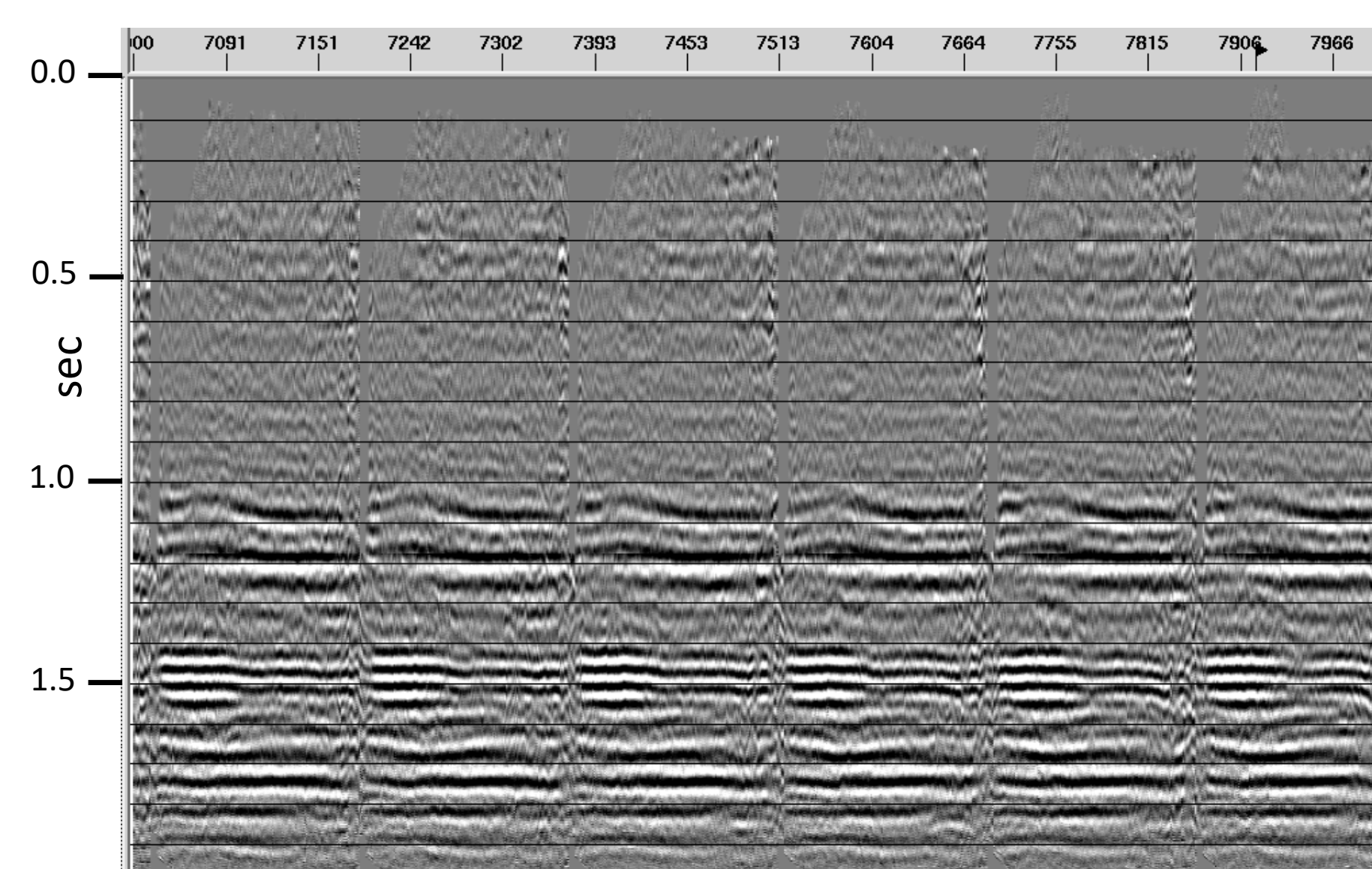


FIG. 7. Six 2D inline slices from the 3D CMP-stacked Blackfoot data volume, **3D raypath interferometry** applied.

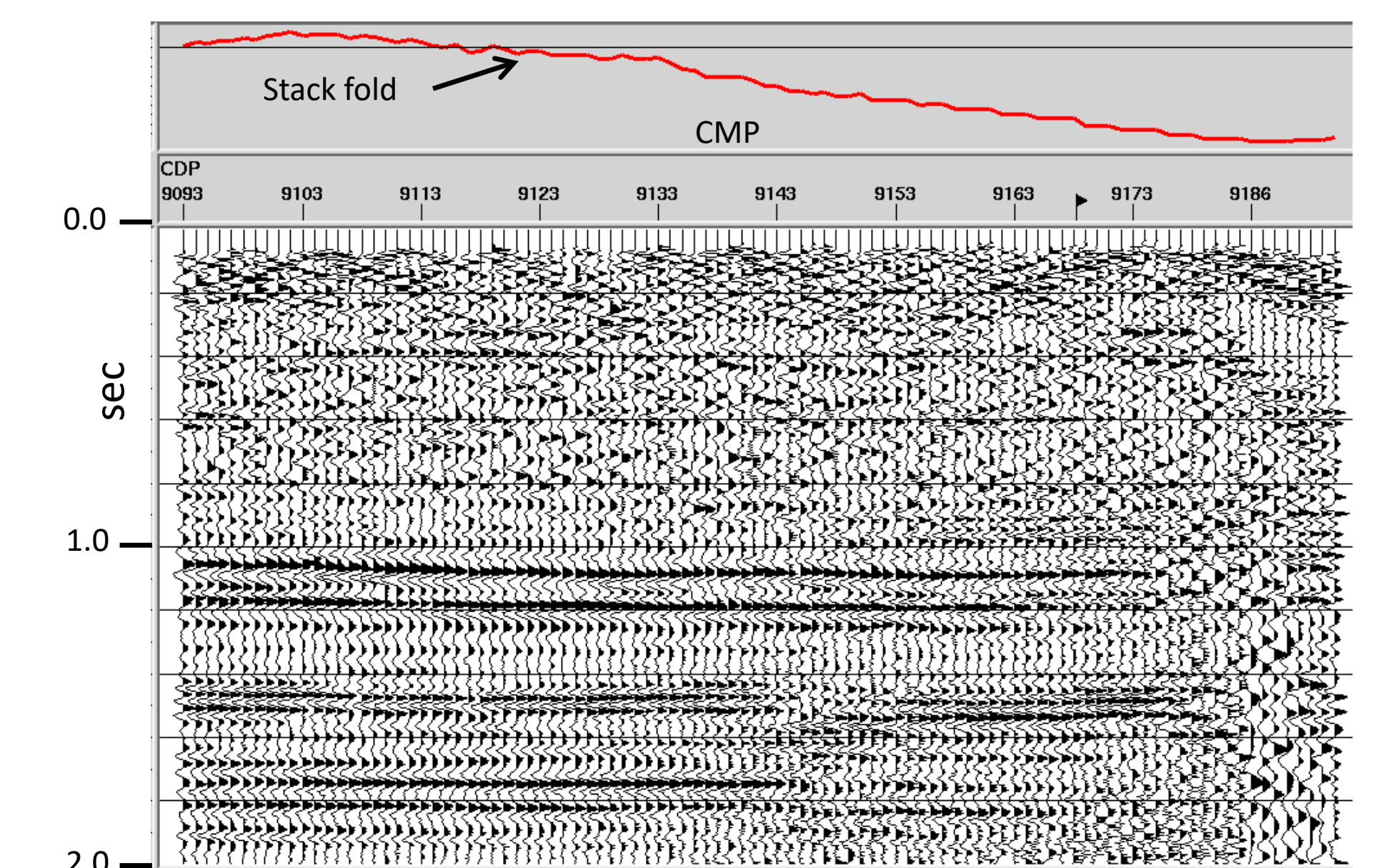


FIG. 8. 2D inline slice from the CMP-stacked Blackfoot PP 3D data volume, no statics applied.

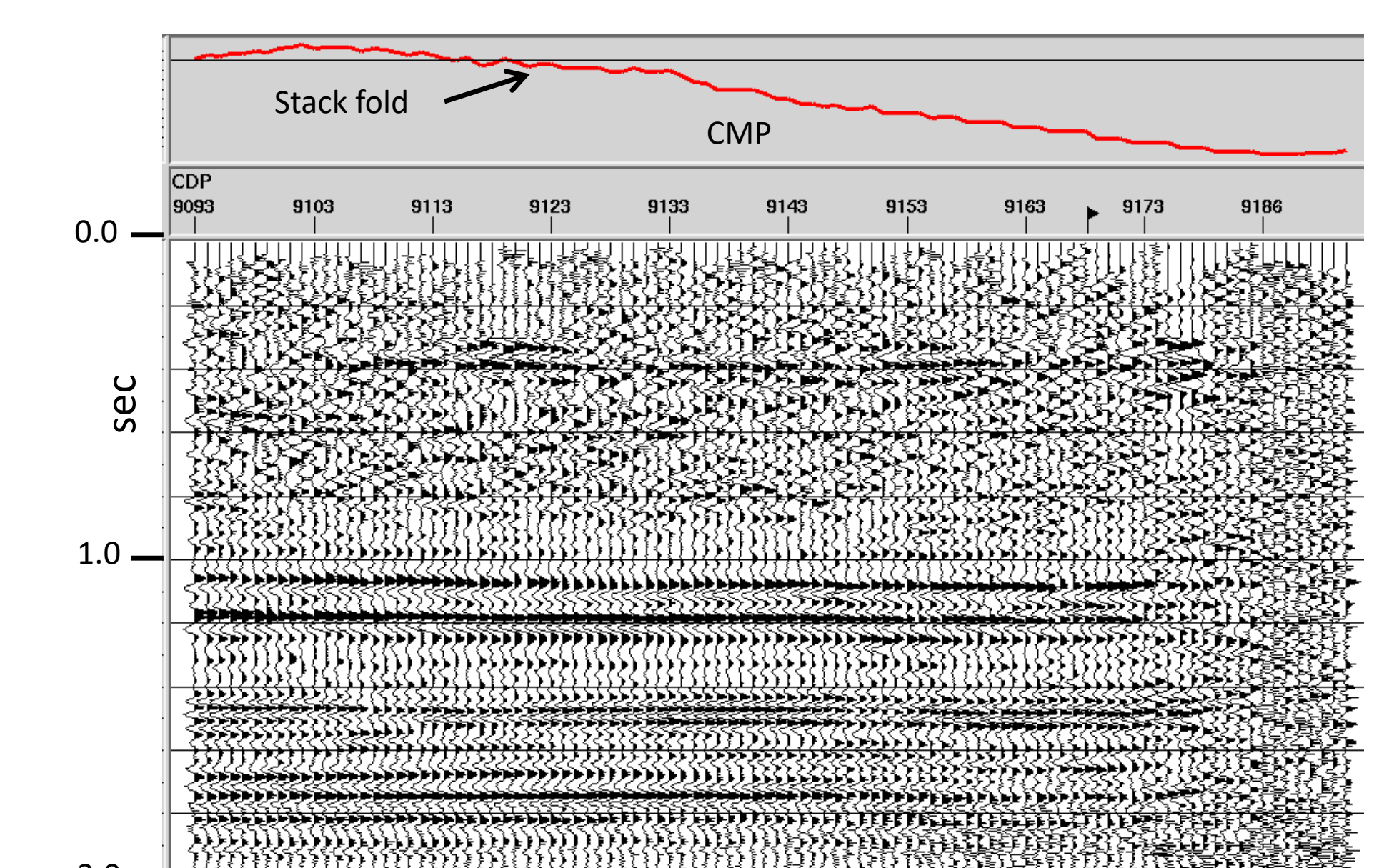


FIG. 9. Same 2D inline slice as Figure 8, **3D raypath interferometry** applied.

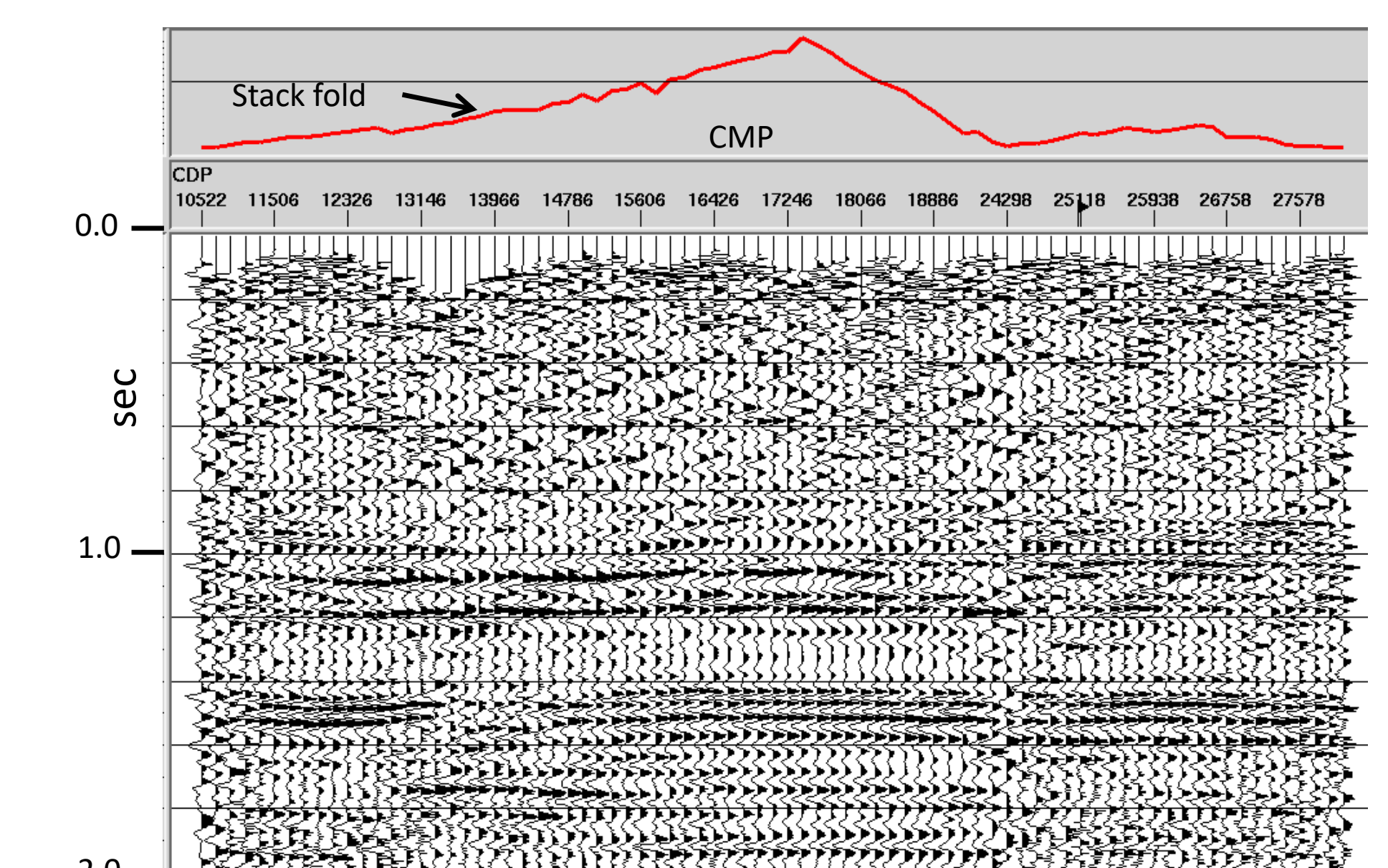


FIG. 10. 2D crossline slice from CMP-stacked Blackfoot PP 3D data volume, no statics applied.

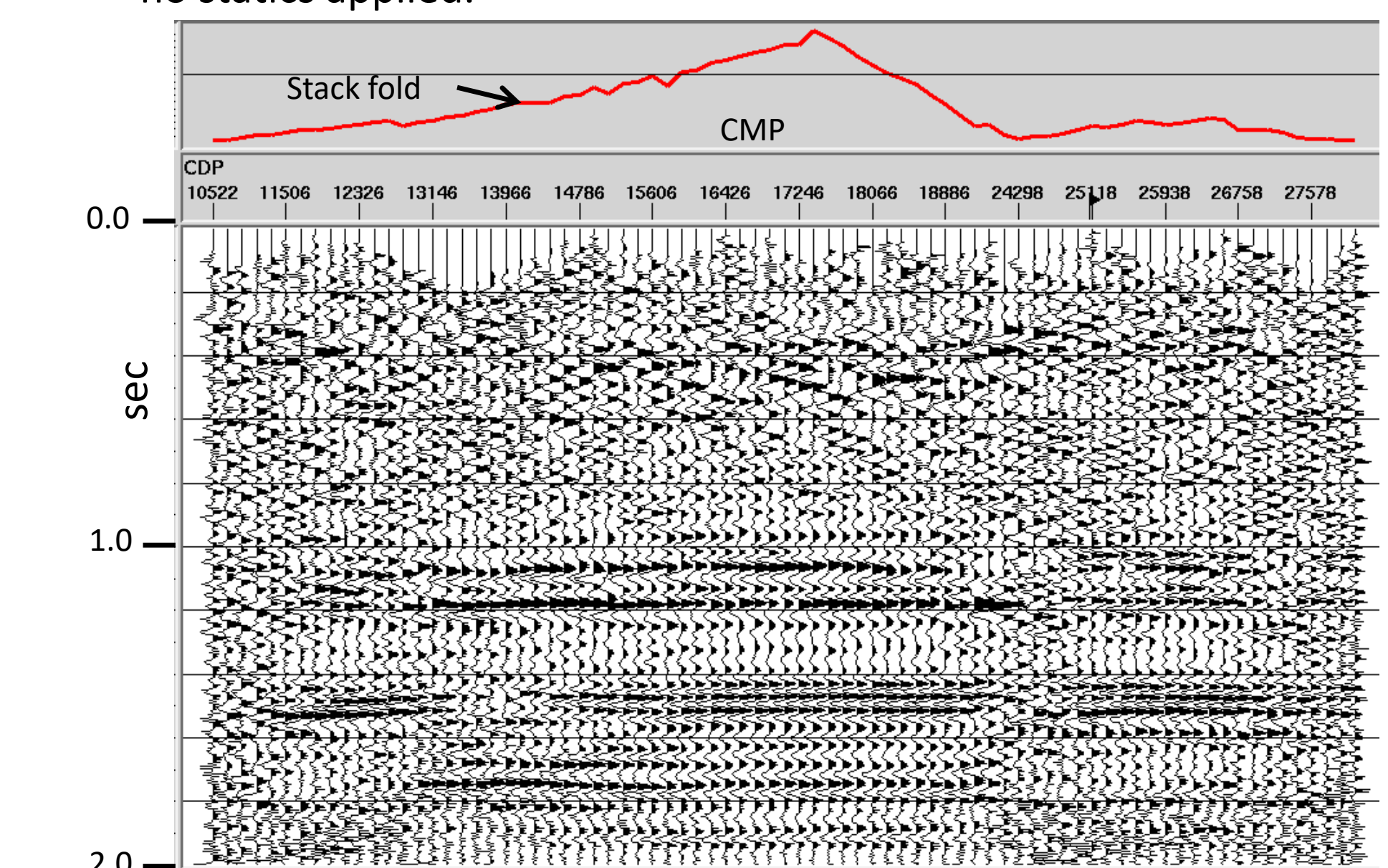


FIG. 11. Same 2D crossline slice as Figure 10, **3D raypath interferometry** applied. 3D raypath interferometry is thus confirmed to be a **true 3D process**.